www.czasopisma.pan.pl PAN POLSKA AKADEMIA NAUK www.journals.pan.pl

jet INTL JOURNAL OF ELECTRONICS AND TELECOMMUNICATIONS, 2020, VOL. 66, NO. 1, PP. 17-23
Manuscript received November 15, 2019; revised January, 2020. DOI: 10.24425/ijet.2019.130260

# Interference in Multi-beam Antenna System of 5G Network

Jan M. Kelner and Cezary Ziółkowski

***Abstract*—Massive multiple-input-multiple-output (MIMO) and beamforming are key technologies, which significantly influence on increasing effectiveness of emerging fifth-generation (5G) wireless communication systems, especially mobile-cellular networks. In this case, the increasing effectiveness is understood mainly as the growth of network capacity resulting from better diversification of radio resources due to their spatial multiplexing in macro- and micro-cells. However, using the narrow beams in lieu of the hitherto used cell-sector brings occurring interference between the neighboring beams in the massive-MIMO antenna system, especially, when they utilize the same frequency channel. An analysis of this effect is the aim of this paper. In this case, it is based on simulation studies, where a multi-elliptical propagation model and standard 3GPP model are used. We present the impact of direction and width of the neighboring beams of 5G new radio gNodeB base station equipped with the multi-beam antenna system on the interference level between these beams. The simulations are carried out for line-of-sight (LOS) and non-LOS conditions of a typical urban environment.**

***Keywords*—5G systems & networks, interference, massive-MIMO, multi-elliptical propagation model, multi-beam antenna system, simulation studies**

## I. Introduction

THE mobile telephony market is on the eve of the introduction of fifth-generation (5G) systems, also called International Mobile Telecommunication (IMT)-2020 [1–3]. However, it should be emphasized that this next stage of evolution is a kind of revolution that covers most of the newly created radiocommunication systems. So, when we talk about 5G wireless systems, we mean not only mobile-cellular systems but also satellite communications, wireless local and sensor networks (WLANs & WSNs), Internet of Things (IoT), machine-to-machine (M2M) and vehicle-to-everything (V2X) communications that including vehicle-to-vehicle (V2V), vehicle-to-pedestrian (V2P), and vehicle-to-infrastructure (V2I) systems. The goal of the next generation of communication systems is to increase their efficiency compared to modern systems. Among the significant benefits, we might mention [1–8]:

- increasing speed to 20 and 10 Gb/s for downlink and uplink transmissions, respectively;
- transmission speeds of 10, 100, and 1000 Mb/s for tens of thousands of users, for metropolitan areas, and for each employee on the same floor of an office building, respectively;
- up to a 10,000-fold increase in network capacity compared to current ones;
- up to a 1000-fold increase in the volume of data per geographical area, e.g. for indoor installations, ultimately up to 10 Mb/s/m$^2$;
- ability to simultaneously support several hundred thousand connections for WSN;
- significantly higher spectral efficiency compared to fourth-generation (4G) systems – up to 30 and 15 bit/s/Hz for down- and uplink, respectively;
- significantly lower latency times, up to 1 ms, compared to Long Term Evolution (LTE), i.e., 4G systems,
- higher speed limit for mobile users - up to 500 km/h;
- greater spatial range of 5G networks;
- improved signaling efficiency.

Not all of the above parameters and functionalities will be implemented in every 5G solution. It is closely related to the so-called usage scenario. Three key services have been identified in 5G and beyond systems:

- enhanced mobile broadband (eMBB),
- massive machine-type communications (mMTC),
- ultra-reliable low latency communications (URLLC),

which define the so-called triangle of potential usage scenarios, shown in Fig. 1 [1].

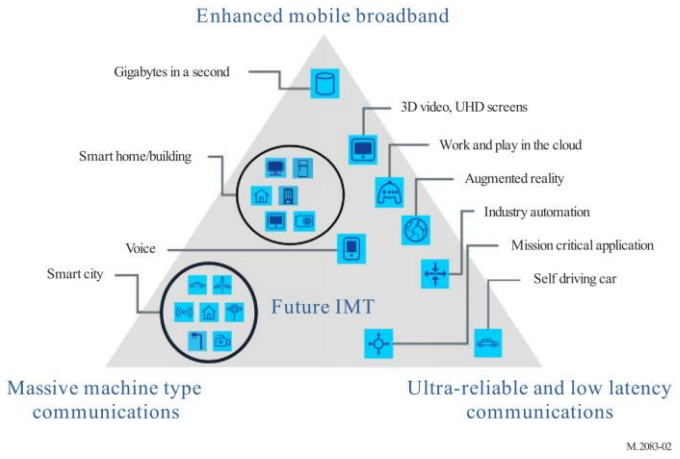


Fig. 1. Usage scenarios for IMT-2020 and beyond.

The introduction of 5G networks and systems is a great challenge primarily for technological reasons. The Ministry of

This work was developed within a framework of the Research Grant "Basic research in sensor technology field using innovative data processing methods" no. GBMON/13-996/2018/WAT sponsored by the Polish Ministry of Defense.

Jan M. Kelner and Cezary Ziółkowski with the Military University of Technology, Faculty of Electronics, Institute of Communications Systems, Gen. Sylwester Kaliski Str. No. 2, 00-908 Warsaw, Poland (e-mail: jan.kelner@wat.edu.pl, cezary.ziolkowski@wat.edu.pl).

Digital Affairs of the Republic of Poland has prepared the document '5G strategy for Poland' [8], which presents the basic assumptions, requirements, possibilities and technologies that will be used in the upcoming new generation systems. Among the key technologies that will achieve the intended goals and technical parameters, multi-antenna array is listed first, especially in the so-called massive multiple-input-multiple-output (MIMO) variant. Other important technologies include software-defined networking (SDN), network functions visualization (NFV), network slicing (NS) mobile edge computing (MEC), fog computing (FC), cloud-radio access network (C-RAN), ultra-dense network (UDN), self-organizing network (SON), multi-radio access technology (Multi-RAT), coordinated multipoint transmission (CoMP). Although many of these technologies have been used for some time, including in 4G systems, they are often defined as 5G technologies.

5G technologies will ensure the increasing effectiveness of emerging systems. In this case, the increasing effectiveness is understood mainly as the growth of network capacity resulting from better diversification of radio resources due to their spatial multiplexing in macro- and micro-cells. However, using the narrow beams in lieu of the hitherto used cell-sector brings occurring interference between the neighboring beams in the massive-MIMO antenna system, especially, when they utilize the same frequency channel. These interferences cause degradation of the quality of service (QoS) [9] and reduction of the downlink capacity [10] in 5G networks. An analysis of this effect is the purpose of this paper. Our evaluation is based on simulation studies, where a multi-elliptical propagation model (MPM) [11–14] and standard model developed by the 3rd Generation Partnership Project (3GPP) [15,16] are used. We present the impact of a direction and half-power beamwidth (HPBW) of the neighboring beams of 5G new radio (NR) gNodeB base station equipped with the massive-MIMO antenna system on the interference level between these beams. The simulations are carried out for line-of-sight (LOS) and non-LOS (NLOS) conditions of a typical urban environment.

The remainder of the paper is organized as follows. A short introduction to multiplexing techniques and MIMO technology is contained in Section II. Section III presents a compact characterization of the MPM. In Section IV, a scenario and assumptions established in simulation studies are described. The analysis of the obtained results is shown in Section V. Summary and final remarks accomplish the paper.

## II. Spatial Multiplexing and Massive-MIMO

Providing end-users with faster speeds and lower transmission delays requires that mobile operators use new techniques and technologies recommended in the 4G and 5G standards. These technologies are implemented primarily on the sides of the gNodeB base station and backbone network. Until now, mobile networks were designed mainly based on macro- and micro-cells. 4G systems provide already support for much smaller pico- and femto-cells [17,18]. These solutions will be implemented on a larger scale only in the coming years as part of 5G networks. Another important change, enabling greater network capacity, is the use of new spectral resources. In addition to the bands used by Global System for the Mobile Communications (GSM), Universal Mobile Telecommunications System (UMTS) and LTE, it is planned to adopt the 700 MHz, 3.6, and 26 GHz bands.

The use of higher frequency ranges is associated with numerous practical problems that mainly result from the nature of radio waves and their interaction with an environment. As the frequency increases, the attenuation of the received signal increases. Thus, the usable spatial range of the radio transmitters decreases. This is the reason for the reduction of cell size and, as a result, an increase in the density of radio network elements (UDN). Communication in urban areas must also be faced with adverse propagation phenomena such as multipath and Doppler effects [19,20]. They contribute to adverse dispersion phenomena in the time, frequency and angle of arrival (AOA) domains of the received signal [14]. To counteract these adverse effects of propagation phenomena and to effectively manage available radio resources, various techniques in signal processing are used in radio communication systems, e.g., convolutional coding, channel equalizers, time- (TDMA), frequency- (FDMA) code- CDMA or space-division multiplexing access (SDMA) [21,22]. Within 5G, it is planned to use various multi-access techniques, including orthogonal frequency-division multiple access (OFDMA), pattern division multiple access (PDMA), multi-user shared access (MUSA) and interleave division multiple access (IDMA), sparse code multiple access (SCMA), and non-orthogonal multiple access (NOMA) [1–8].

The SDMA is closely related to antenna technology. In older generations of cell networks, sector antennas are mainly used. In 4G and modern Wi-Fi networks, the MIMO and multi-user MIMO (MU-MIMO) techniques are increasingly used. Their effectiveness is noticeable above all in a multipath propagation environment [23,24]. In 5G, it is planned to use a more advanced version of MIMO, i.e., massive-MIMO [25][26], and beamforming [27][28]. A certain version of massive-MIMO, also called full-dimensional MIMO (FD-MIMO), has already been proposed in currently used LTE-Advance Pro (LTE-A Pro) systems [29,30]. These modern technologies allow to reduce dispersion in the received signal, especially in the AOA-domain, and to provide the spatial multiplication of available radio resources.

In 5G mobile networks, significant changes in antenna techniques will occur mainly in the macro-cell gNodeB based stations. In older generation systems, the macro-cell was usually divided into three 120° angular sectors. To provide coverage in the sector, one or two sectoral antennas with the HPBW equal to 120° or 60° are used, respectively. In LTE and LTE-A, the antennas were already based on MIMO and MU-MIMO technologies. LTE-A Pro standard also allowed the use of FD-MIMO technology. In 5G, macro-cell base station antennas will be based on efficient massive-MIMO technology. A comparison of macro-cell user service methods using sector antennas and massive-MIMO antennas is shown in Figure 2 (based on [27]). This is a typical application of the massive-MIMO technology in the macro-cell gNodeB, where the sector will be divided into smaller angular sections, i.e., beams. Other scenarios for using the massive-MIMO are presented, i.a., in [14,26].

A comparison of user service methods pursued by base stations of macro-cells using the sectoral and massive-MIMO antenna systems is shown in Fig. 2 (based on [31]). This is a typical application of massive-MIMO technology in the macro-

cell gNodeB, where the sector will be divided into smaller angular sections, i.e., beams. Other scenarios for using massive-MIMO are presented, i.a., in [30].

Massive-MIMO technology is based on utilizing the antenna arrays with a large number of antenna elements. Depending on the needs and application scenario, these antenna arrays may be, e.g., planar or cylindrical. Figure 3 presents three typical solutions of planar arrays in the form of a matrix, as well as a vertical, or horizontal antenna patch. In the general case, in the 5G NR base stations, it is planned to use the matrix antenna arrays directed at the individual sectors of the macro-cell. It may be three or four sectors. A large number of antenna elements makes it possible to generate really narrow beams both in the azimuth ($\varphi$) and elevation ($\theta$) planes. In some scenarios, it may be more beneficial to use the vertical or horizontal antenna patches. The vertical antenna patches give the possibility of generating narrow beams in the elevation plane and wider in the azimuth plane ($HPBW_\theta < HPBW_\varphi$). Therefore, these antenna patches are used when diversification of the beams in the elevation plane is necessary. The opposite case is for the horizontal patches, ti.e. the generated beams are wider in the elevation than in the azimuth plane ($HPBW_\theta > HPBW_\varphi$). Thus, they ensure diversification in the azimuth plane.

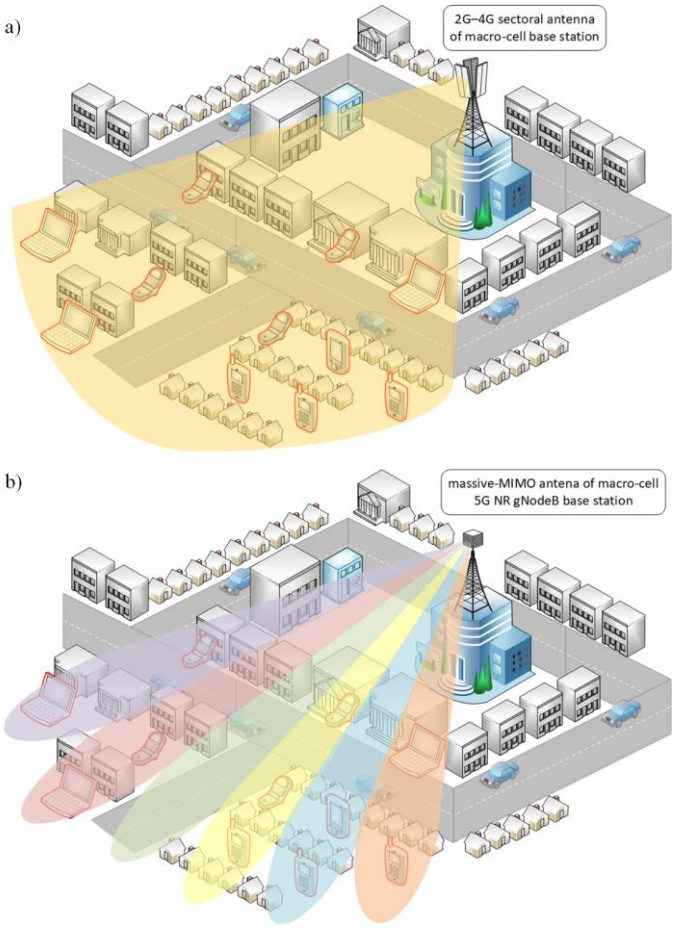


Fig. 2. Coverage of macro-cell sector by a) wideband sectoral antenna beam and b) narrowband antenna beam made in massive-MIMO technology.

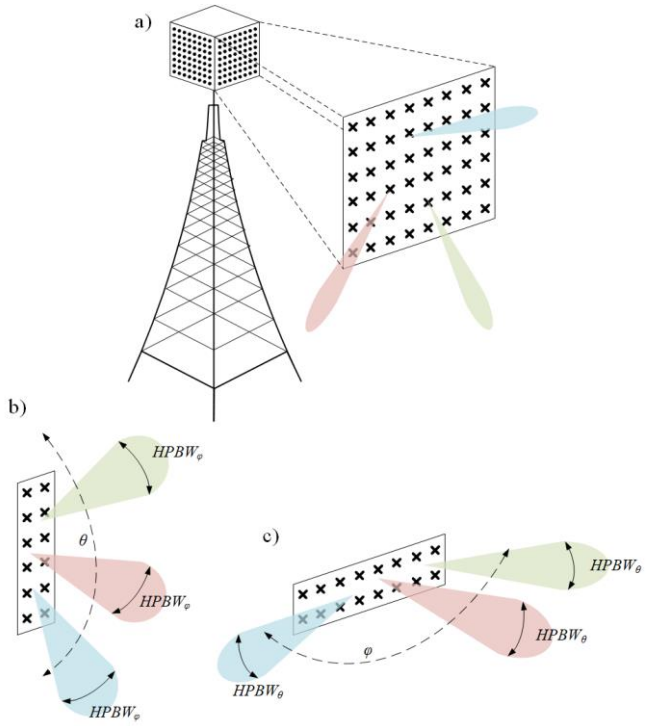


Fig. 3. Planar arrays in form of a) antenna matrix, b) vertical, or c) horizontal antenna patch.

## III. Multi-Elliptical Propagation Model

The MPM is a geometry-based statistical model (GBSM). In this case, a multi-elliptical structure representing the potential locations of scatterers and delays of signal components in a multipath propagation environment, which is illustrated in Fig. 4 [11–14].

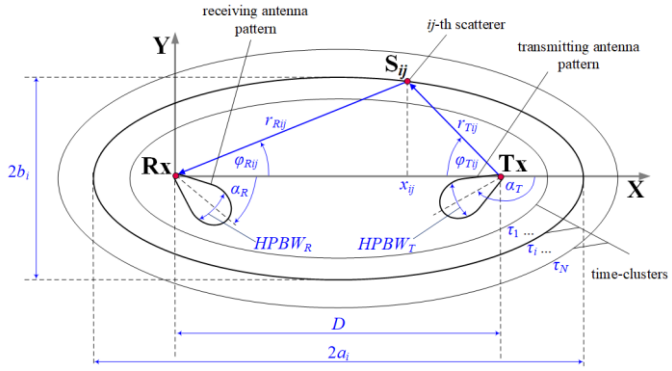


Fig. 4. Scattering geometry of MPM.

The MPM is based on the multi-elliptical Parsons–Bajwa [32] and Oestges–Erceg–Paulraj [33] models. A common feature of these models is the relationship between the characteristic delays occurring in a power delay profile (PDP) and the dimensions of the confocal ellipses forming the geometric structure of these models. The MPM also includes local scattering occurring around the transmitting and receiving antennas. For this purpose, the von Mises distribution is used [34]. Additionally, the MPM is one of the few models that allows considering the transmitting and receiving antenna patterns. In that, the directional beams of the multi-antenna systems might be also modeled.

The MPM in the presented version is a two-dimensional (2D) model that only considers the azimuth plane. The three-dimensional (3D) version of the MPM, i.e., considering also the elevation plane, is presented in [13,35,36]. In this case, the scattering areas of delayed components are represented by the structure of confocal semi-ellipsoids.

The MPM gives the ability to determine a power angular spectrum (PAS), $P_R$, as a function of the azimuth angle, $\varphi$, PDP, distance $D$ between the transmitter (Tx) and the receiver (Rx), HPBWs, maximum directions of radiation, $\alpha_T$, and reception, $\alpha_R$, of the transmitting and receiving antennas (see Fig. 4), respectively:

$$P_R(\varphi) = P_R(\varphi, P_i, \tau_i, D, HPBW_T, \alpha_T, HPBW_R, \alpha_R) \tag{1}$$

where $(P_i, \tau_i)$, $i = 0, 1, \ldots, N$, represent characteristic powers and delays of $N + 1$ time-clusters occurring in the PDP, i.e, in the analyzed propagation environment.

A detailed description of the MPM and calculation method of the PAS are presented in [11–14] and [13,35,36] for the 2D and 3D versions of the model, respectively.

## IV. Scenario and Assumptions for Simulation Studies

In the simulation studies, we assume the scenario of using the massive-MIMO multi-beam system similar to the one presented in Fig. 2b. This means that the macro-cell gNodeB base station generates adjacent beams in the azimuth plane that cover the cell sector. Figure 5 depicts the detailed scenario of the simulation tests.

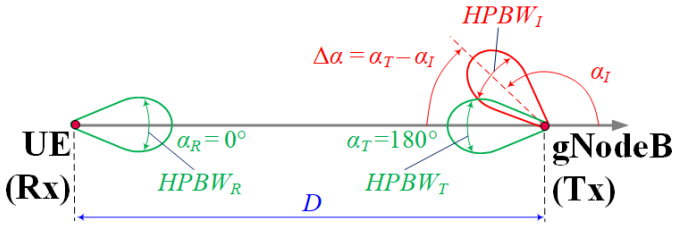


Fig. 5. Spatial scenario of simulation studies.

In the analyzed case, the gNodeB generates the beam (green color) with $HPBW_T$ towards a mobile station so-called a user equipment (UE), i.e., $\alpha_T = 180°$. The UE antenna beam with $HPBW_R$ is directed towards the gNodeB, i.e., $\alpha_R = 0°$. The base station also generates other beams (red color) with $HPBW_I = HPBW_T$ whose maximum radiation direction is equal to $\alpha_I$. These beams serving a different area of the sector may cause interference in the UE. In this case, we assume that each of the two analyzed gNodeB beams will use the same spectral resources, i.e., the frequency channel. In the simulation studies, we assess the impact of a separation angle of the beams, $\Delta\alpha = \alpha_T - \alpha_I$, in the base station on the interference level in the signal received by the UE. The tests are carried out for selected values of $D$, $HPBW_T$, $HPBW_R$, and for LOS and NLOS propagation conditions between the transmitting (gNodeB) and receiving (UE) antennas.

In the simulation tests, we consider the following assumptions:

- carrier frequency of the transmitted signal is equal to $f_0 = 3.6$ GHz,
- considered PDPs are based on TDL-D and TLD-B, i.e., tapped-delay line (TDL) models of the 3GPP standard [15,16] for LOS and NLOS conditions, respectively,
- these TDLs correspond an urban macro (UMa) scenario and normal-delay profile, i.e., rms delay spread is equal to $\sigma_\tau = 363$ ns [15,16],
- Rician factor depicting the power division of the 0th time-cluster between a direct path and the local scattering components, is equal to $\kappa = 21.4$ (13.3 dB) or $\kappa = 0$ [15,16] for LOS or NLOS conditions, respectively,
- coefficient of the von Mises distribution illustrating the intensity of the local scattering is equal to $\gamma = 0$,
- analyzed distances between the gNodeB (Tx) and UE (Rx) are equal to $D_1 = 100$ m and $D_2 = 500$ m,
- considered the following HPBWs of the gNodeB beam, $HPBW_T$, 10°, 20°, or 30°,
- HPBW of the interfering beams is $HPBW_I = HPBW_T$,
- following HPBWs of the UE antenna beam is analyzed 30°, 60°, or 360°.

## V. Analysis of Simulation Results

### A. Measure of Interference

In the analysis of the influence of the multi-beam antenna system on the interference level from the neighboring beam, a measure of a signal-to-interference ratio (SIR) is used

$$SIR[\text{dB}] = 10\log_{10}\frac{P_S}{P_I} \tag{2}$$

where $P_S$ and $P_I$ are powers of useable and interference signals induced in the UE receiving antennas transmitted by the correct subscriber-beam and neighboring interfering-beams, respectively.

These powers are determined based on two PASs obtained by the MPM for the subscriber beam ($\alpha_T = 180°$, $\alpha_R = 0°$) and the interfering beam ($\alpha_{TI} = \alpha_T - \Delta\alpha$, $\alpha_R = 0°$), respectively,

$$P_S = \int_{-180°}^{+180°} P_R(\varphi, P_i, \tau_i, D, HPBW_T, \alpha_T, HPBW_R, \alpha_R)\,\mathrm{d}\varphi \tag{3}$$

$$P_I = \int_{-180°}^{+180°} P_R(\varphi, P_i, \tau_i, D, HPBW_I, \alpha_I, HPBW_R, \alpha_R)\,\mathrm{d}\varphi \tag{4}$$

For such the defined issue (see Fig. 5), the interfering and subscriber beams are from the same antenna system. Therefore, for $\Delta\alpha = 0$, we have $P_S = P_I$. This means that $SIR = 0$ dB.

Based on the simulation results, we have carried out the impact evaluation of the separation angle, $\Delta\alpha$, and the HPBWs of antenna beams on the SIR. The obtained results are presented in Figs. 6–13, whereby Figs. 6–9 refer to different HPBWs of the gNodeB transmitting beams, whereas, the impact of $HPBW_R$ on the SIR is shown in Figs. 10–13. In the simulation studies, the effects of propagation phenomena under LOS and NLOS conditions for two different Tx-Rx distances are also included.

### B. Impact of Transmitting Antenna HPBW

Figures 6–9 illustrate the effect of $HPBW_T$ changes on the SIR as a function of the separation angle for $HPBW_R = 60°$.

The results for LOS conditions presented in Figs. 6 and 7 show, as expected, an increase in the SIR along with a decrease in the concurrence between the radiation direction of the interfering beam and the Tx-Rx direction. After exceeding the value corresponding to approximately $\Delta\alpha = 1.5 \cdot HPBW_T$, the dynamics of changes in the interfering signal level decreases. The range of these changes is clearly greater for $D = 500$ m (Fig. 7) and is about 6 dB, while for $D = 100$ m (Fig. 6) it reaches not more than 4 dB.

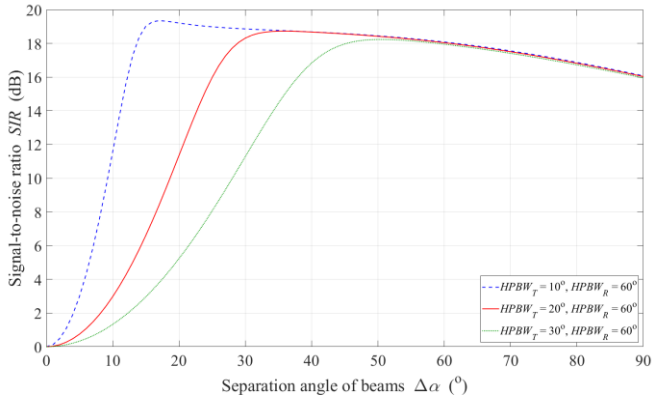


Fig. 6. SIR versus separation angle of beams for LOS conditions, $D$ = 100 m, $HPBW_R$ = 60º, and selected values of $HPBW_T$.

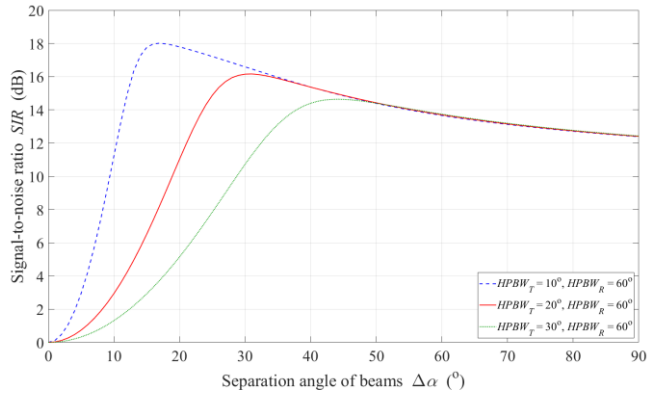


Fig. 7. SIR versus separation angle of beams for LOS conditions, $D$ = 500 m, $HPBW_R$ = 60º, and selected values of $HPBW_T$.

Under NLOS conditions (see Figs. 8 and 9), there are significant differences in the SIR changes as a function of $\Delta\alpha$. The graphs show that as the separation angle increases, there is an increase in the interference level. However, for small distances and narrow patterns of the antenna beams, we may observe the occurrence of an optimal separation angle of about 9°, for which we obtain the maximum SIR of about 5 dB. These results reflect the actual propagation phenomena that we face in the analyzed scenario, e.g., [37,38]. In this case, the propagation paths that reach the Rx from directions significantly diverging from the Tx-Rx direction are dominant.

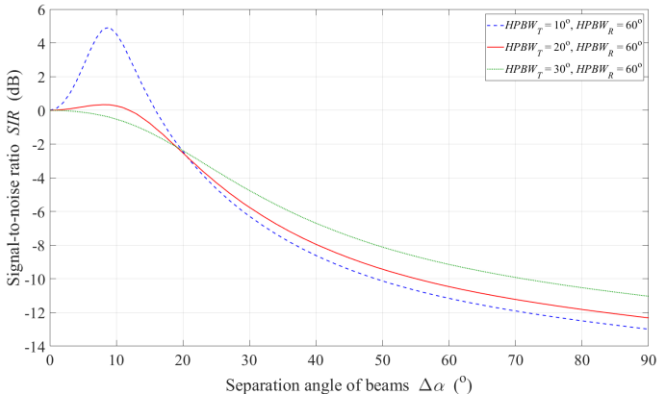


Fig. 8. SIR versus separation angle of beams for NLOS conditions, $D$ = 100 m, $HPBW_R$ = 60º, and selected values of $HPBW_T$.

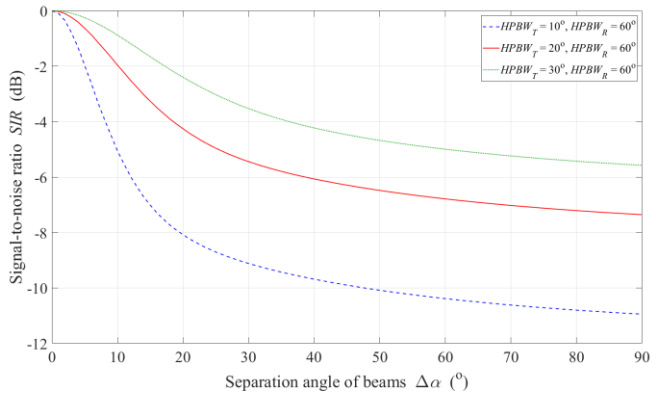


Fig. 9. SIR versus separation angle of beams for NLOS conditions, $D$ = 500 m, $HPBW_R$ = 60º, and selected values of $HPBW_T$.

## C. *Influence of Receiving Antenna HPBW*

Figures 10–13 depict the effect of $HPBW_R$ changes on the SIR as a function of $\Delta\alpha$ for $HPBW_T$ = 10º.

For LOS conditions (see Figs. 10 and 11), we can observe the stabilization of the SIR changes for $\Delta\alpha \approx 15°$. This effect occurs for the analyzed distances and all the receiving antenna HPBWs (30°, 60°, and 360°). In this case, the low $HPBW_R$ ensures an increase of the SIR to 22 dB and 19 dB for the Tx-Rx distance equal to 100 m and 500 m, respectively.

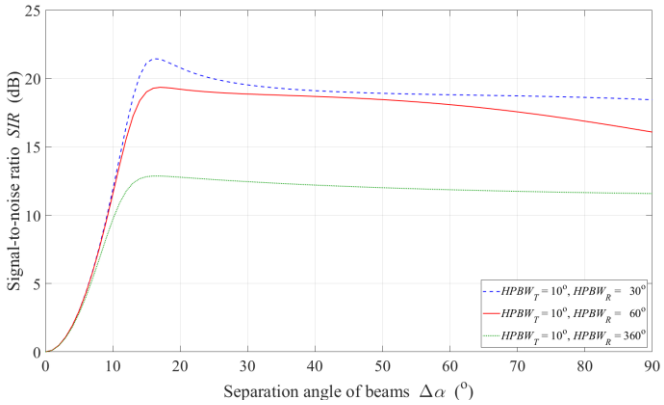


Fig. 10. SIR versus separation angle of beams for LOS conditions, $D$ = 100 m, $HPBW_T$ = 10º, and selected values of $HPBW_R$.

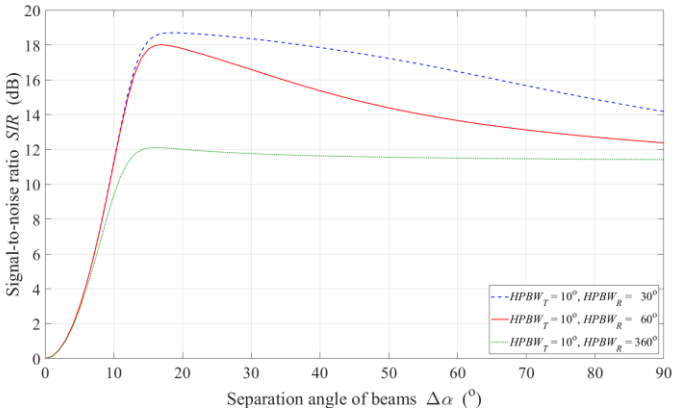


Fig. 11. SIR versus separation angle of beams for LOS conditions, $D$ = 500 m, $HPBW_T$ = 10º, and selected values of $HPBW_R$.

For NLOS conditions (see Figs. 12 and 13), the impact of HPBWR changes on the SIR is analogous to $HPBW_T$ changes described in Section V.B. In this case, we might also observe the occurrence of the optimal value of $\Delta\alpha$, which is about 12º for $D = 100$ m. This separation angle value provides $SIR = 14$ dB.

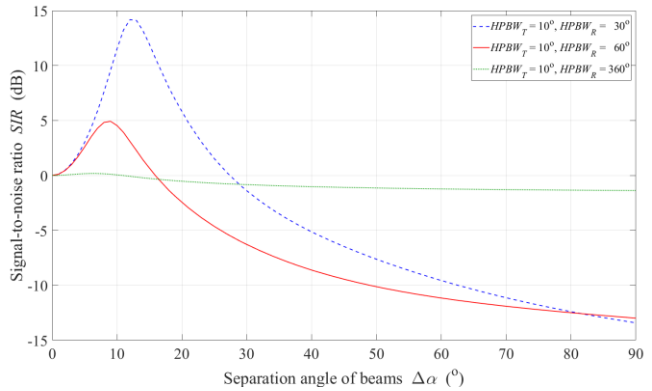


Fig. 12. SIR versus separation angle of beams for NLOS conditions, $D = 100$ m, $HPBW_T = 10º$, and selected values of $HPBW_R$.

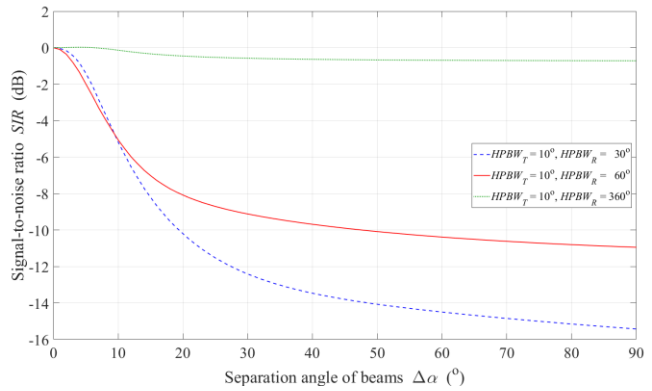


Fig. 13. SIR versus separation angle of beams for NLOS conditions, $D = 500$ m, $HPBW_T = 10º$, and selected values of $HPBW_R$.

Obtained results show that proper selection of parameters of radiation and reception patterns of the antennas can ensure spatial selection of co-band radio channels. The way we select these parameters is presented in the paper.

## VI. Conclusions

The paper is focused on assessing the impact of the multi-beam antenna system on the interference level in the subscriber channel. We show the issues of using the massive-MIMO antenna systems in 5G networks. The basis of the carried out analysis is the simulation studies using the MPM and 3GPP standard model for different antenna parameter configurations and propagation conditions. The obtained results are a premise for using the presented methodology to design directional wireless links based on the multi-beam antennas.

## References

[1] ITU-R, "Recommendation ITU-R M.2083-0: IMT Vision – Framework and overall objectives of the future development of IMT for 2020 and beyond," International Telecommunication Union (ITU), Geneva, Switzerland, Rec. ITU-R M.2083-0, Sep. 2015.

[2] M. Sauter, *From GSM to LTE-Advanced Pro and 5G: An introduction to mobile networks and mobile broadband*, 3rd ed. Hoboken, NJ, USA: Wiley, 2017.

[3] R. Vannithamby and S. Talwar, Eds., *Towards 5G: Applications, requirements and candidate technologies*. Chichester, West Sussex, UK: Wiley, 2017.

[4] A. Gupta and R. K. Jha, "A survey of 5G network: Architecture and emerging technologies," *IEEE Access*, vol. 3, pp. 1206–1232, 2015. DOI: 10.1109/ACCESS.2015.2461602.

[5] M. Agiwal, A. Roy, and N. Saxena, "Next generation 5G wireless networks: A comprehensive survey," *IEEE Commun. Surv. Tutor.*, vol. 18, no. 3, pp. 1617–1655, 2016. DOI: 10.1109/COMST.2016.2532458.

[6] D. Muirhead, M. A. Imran, and K. Arshad, "A survey of the challenges, opportunities and use of multiple antennas in current and future 5G small cell base stations," *IEEE Access*, vol. 4, pp. 2952–2964, 2016. DOI: 10.1109/ACCESS.2016.2569483.

[7] N. Panwar, S. Sharma, and A. K. Singh, "A survey on 5G: The next generation of mobile communication," *Phys. Commun.*, vol. 18, pp. 64–84, Mar. 2016. DOI: 10.1016/j.phycom.2015.10.006.

[8] "5G strategy for Poland," Polish Ministry of Digital Affairs, Warsaw, Poland, Jan. 2018.

[9] F. Qamar, M. N. Hindia, T. Abbas, K. B. Dimyati, and I. S. Amiri, "Investigation of QoS performance evaluation over 5G network for indoor environment at millimeter wave bands," *Int. J. Electron. Telecommun.*, vol. 65, no. 1, pp. 95–101, Feb. 2019. DOI: 10.24425/ijet.2019.126288.

[10] J. M. Kelner, C. Ziółkowski, and L. Nowosielski, "Degradation of radio link capacity with directional antennas," in *2018 40th Progress in Electromagnetics Research Symposium (PIERS)*, Toyama, Japan, 2018, pp. 1791–1796. DOI: 10.23919/PIERS.2018.8598199.

[11] C. Ziółkowski, J. M. Kelner, L. Nowosielski, and M. Wnuk, "Modeling the distribution of the arrival angle based on transmitter antenna pattern," in *2017 11th European Conference on Antennas and Propagation (EuCAP)*, Paris, France, 2017, pp. 1582–1586. DOI: 10.23919/EuCAP.2017.7928823.

[12] J. M. Kelner and C. Ziółkowski, "Modeling power angle spectrum and antenna pattern directions in multipath propagation environment," in *2018 12th European Conference on Antennas and Propagation (EuCAP)*, London, UK, 2018, pp. 1–5. DOI: 10.1049/cp.2018.1268.

[13] J. M. Kelner and C. Ziółkowski, "Multi-elliptical geometry of scatterers in modeling propagation effect at receiver," in *Antennas and wave propagation*, P. Pinho, Ed. London, UK: InTech, 2018, pp. 115–141. DOI: 10.5772/intechopen.75142.

[14] J. M. Kelner and C. Ziółkowski, "Mitigation of angular dispersion in 5G cellular networks," *Elektron. Konstr. Technol. Zastos.*, vol. 60, no. 2, pp. 13–20, Feb. 2019. DOI: 10.15199/13.2019.2.2. (in Polish)

[15] 3GPP, "Study on channel model for frequencies from 0.5 to 100 GHz," 3rd Generation Partnership Project (3GPP), Technical Specification Group Radio Access Network, Valbonne, France, Tech. Rep. 3GPP TR 38.901 V15.0.0 (2018-06), Release 15, Jun. 2018.

[16] 3GPP, "5G. Study on channel model for frequencies from 0.5 to 100 GHz (3GPP TR 38.901 version 15.0.0 Release 15)," European Telecommunications Standards Institute (ETSI), Sophia-Antipolis, France, ETSI TR 138 901 V15.0.0, Jul. 2018.

[17] C. Cox, *An introduction to LTE: LTE, LTE-Advanced, SAE, VoLTE and 4G mobile communications*, 2nd ed. Chichester, West Sussex, UK; Hoboken, NJ, USA: Wiley, 2014.

[18] M. U. Rehman and G. A. Safdar, Eds., *LTE communications and networks: Femtocells and antenna design challenges*. Hoboken, NJ, USA: Wiley, 2018.

[19] N. Blaunstein, *Radio propagation in cellular networks*. Boston, MA, USA: Artech House Publishers, 2000.

[20] R. Vaughan and J. Bach Andersen, *Channels, propagation and antennas for mobile communications*. London, UK: Institution of Engineering and Technology, 2003.

[21] A. F. Molisch, *Wireless communications*, 2nd ed. Chichester, West Sussex, U.K: Wiley-IEEE Press, 2010.

[22] T. S. Rappaport, *Wireless communications: Principles and practice*, 2nd ed. Upper Saddle River, NJ, USA: Prentice Hall, 2002.

[23] M. M. da Silva and F. A. Monteiro, Eds., *MIMO processing for 4G and beyond: Fundamentals and evolution*. Boca Raton, FL, USA: CRC Press, 2014.

[24] C. Wang, *Adaptive downlink multi-user MIMO wireless systems: Investigations, analyses, strategies*. Saarbrücken, Germany: VDM Verlag Dr. Müller, 2008.

[25] S. A. Busari, K. M. S. Huq, S. Mumtaz, L. Dai, and J. Rodriguez, "Millimeter-wave massive MIMO communication for future wireless systems: A survey," *IEEE Commun. Surv. Tutor.*, vol. 20, no. 2, pp. 836–869, 2018. DOI: 10.1109/COMST.2017.2787460.

[26] T. L. Marzetta, E. G. Larsson, H. Yang, and H. Q. Ngo, *Fundamentals of massive MIMO*. Cambridge, UK; New York, NY, USA: Cambridge University Press, 2016.

[27] S. Kutty and D. Sen, "Beamforming for millimeter wave communications: An inclusive survey," *IEEE Commun. Surv. Tutor.*, vol. 18, no. 2, pp. 949–973, 2016. DOI: 10.1109/COMST.2015.2504600.

[28] W. Liu and S. Weiss, *Wideband beamforming: Concepts and techniques*. Chichester, West Sussex, UK: Wiley, 2010.

[29] H. Ji *et al.*, "Overview of full-dimension MIMO in LTE-Advanced Pro," *IEEE Commun. Mag.*, vol. 55, no. 2, pp. 176–184, Feb. 2017. DOI: 10.1109/MCOM.2016.1500743RP.

[30] Y. Kim *et al.*, "Full dimension MIMO (FD-MIMO): The next evolution of MIMO in LTE systems," *IEEE Wirel. Commun.*, vol. 21, no. 2, pp. 26–33, Apr. 2014. DOI: 10.1109/MWC.2014.6812288.

[31] "Mitsubishi Electric's new multibeam multiplexing 5G technology achieves 20Gbps throughput," Mitsubishi Electric Corporation, Tokyo, Japan, 2984, Jan. 2016.

[32] J. D. Parsons and A. S. Bajwa, "Wideband characterisation of fading mobile radio channels," *IEE Proc. F Commun. Radar Signal Process.*, vol. 129, no. 2, pp. 95–101, Apr. 1982. DOI: 10.1049/ip-f-1:19820016.

[33] C. Oestges, V. Erceg, and A. J. Paulraj, "A physical scattering model for MIMO macrocellular broadband wireless channels," *IEEE J. Sel. Areas Commun.*, vol. 21, no. 5, pp. 721–729, Jun. 2003. DOI: 10.1109/JSAC.2003.810322.

[34] A. Abdi, J. A. Barger, and M. Kaveh, "A parametric model for the distribution of the angle of arrival and the associated correlation function and power spectrum at the mobile station," *IEEE Trans. Veh. Technol.*, vol. 51, no. 3, pp. 425–434, May 2002. DOI: 10.1109/TVT.2002.1002493.

[35] C. Ziółkowski and J. M. Kelner, "Antenna pattern in three-dimensional modelling of the arrival angle in simulation studies of wireless channels," *IET Microw. Antennas Propag.*, vol. 11, no. 6, pp. 898–906, May 2017. DOI: 10.1049/iet-map.2016.0591.

[36] C. Ziółkowski and J. M. Kelner, "Statistical evaluation of the azimuth and elevation angles seen at the output of the receiving antenna," *IEEE Trans. Antennas Propag.*, vol. 66, no. 4, pp. 2165–2169, Apr. 2018. DOI: 10.1109/TAP.2018.2796719.

[37] J. Lee, M.-D. Kim, J.-J. Park, and Y. J. Chong, "Field-measurement-based received power analysis for directional beamforming millimeter-wave systems: Effects of beamwidth and beam misalignment," *ETRI J.*, vol. 40, no. 1, pp. 26–38, Feb. 2018. DOI: 10.4218/etrij.2017-0188.

[38] M.-D. Kim, J. Liang, J. Lee, J. Park, and B. Park, "Directional multipath propagation characteristics based on 28GHz outdoor channel measurements," in *2016 10th European Conference on Antennas and Propagation (EuCAP)*, 2016, pp. 1–5. DOI: 10.1109/EuCAP.2016.7481755.